Vectors, components, and minerals

Donald M. Burt

Department of Geology, Arizona State University, Tempe, Arizona 85287-1404, U.S.A.

Abstract

Ionic substitutions in minerals are directed chemical displacements and may be treated as vector quantities. This approach, pioneered by J. V. Smith and J. B. Thompson, Jr., has many advantages over the barycentric coordinates (such as Gibbs triangles) long familiar to mineralogists and petrologists. Among these are the convenience of plotting recalculated mineral formulas directly on x-y (cartesian) diagrams; a possible reduction in the number of end-members, e.g., in the spinel and garnet groups, resulting from the valence insensitivity of exchange operators; the identification of possible new end-members, illustrated with composition planes that have up to five vertices; and the applicability of the same set of vectors to different minerals, illustrated with regard to pyroxene, plagioclase, and melilite.

Planar vector diagrams for a given mineral group can have chemical limits, generally dictated by ionic charge and bounded by lines representing zero contents of individual ions, as well as narrower crystal-chemical limits, generally dictated by ionic radii and bounded by lines representing constraints such as all Si as tetrahedral and Mg as octahedral. A given vector does not necessarily imply that a given mineral will be correspondingly zoned chemically, unless the mineral's composition is very close to a chemical or crystal-chemical limit.

Introduction

Geologists conventionally plot mineral and rock compositions on triangles; the suggestion to plot compositions according to a center of gravity (barycentric coordinates) was made by J. W. Gibbs in 1878 (reprinted in Gibbs, 1906, 1961, p. 118). J. B. Thompson, Jr. (1981, p. 159) cites W. L. Bragg (1937; cf. Bragg et al., 1965, p. 23) for first suggesting that the compositions of complex mineralogical solid solutions could be represented by the extent of substitutions from a given end-member composition rather than by proportions of a bewildering variety of individual end-members. This approach was used by Smith (1959) for model amphibole compositions and, much amplified, by Thompson (1981, 1982) for amphiboles and other minerals.

Ionic substitutions in minerals, generally represented by an undirected notation such as Na + Si = Ca + Al (e.g., for plagioclase), can be represented more succinctly by directed exchange operators (Burt, 1974) such as $NaSi(CaAl)_{-1}$. This notation for the operation of ionic exchange was introduced in class lectures in the late 1960s by J. B. Thompson, Jr. My initial interest in exchange operators (Burt, 1974, 1979) was prompted by the realization that they must be intrinsically acidic or basic in the electronic or Lewis (1938) sense, because different ions possess different electronic environments. For many years, exchange operators were used barycentrically (as points on triangles) or algebraically or in terms of their chemical potentials ("exchange potentials"), rather than

as composition vectors. My first use of composition vectors was in a systematization of lithium micas (in Černý and Burt, 1984). Independent ionic substitutions in minerals, such as in this case $LiAlFe_{-2}$ and $FeSiAl_{-2}$, are directed chemical displacements (i.e., they have both a direction and a magnitude) and are as much vectors as physical displacement operations (cf. Hoffmann, 1966, 1975). The starting point for chemical displacement operations was termed the "additive component" by Thompson (1981, 1982).

The unique feature of my vector diagrams was that they included a scaled vector inset that showed the algebraic relations among various ionic substitutions graphically. Individual vectors on this scaled inset can be labeled by ions that are not involved in the substitution and are constant along their length. Their slopes correspond with the slopes of isocomposition lines on the associated composition diagram. This labeling of vectors by noninvolved ions is somewhat analogous to the labeling of univariant lines around an invariant point by noninvolved phases (e.g., Zen, 1966), and it can be extended into the third dimension.

This vector approach has also been applied to phyllosilicates in general (Burt, 1988), to tourmaline (Burt, 1989a), and to a large variety of rare earth–bearing minerals (Burt, 1989b). The purpose of this article is to make some generalizations based on this previous work and to give additional examples of the application of vector diagrams to several mineral groups.
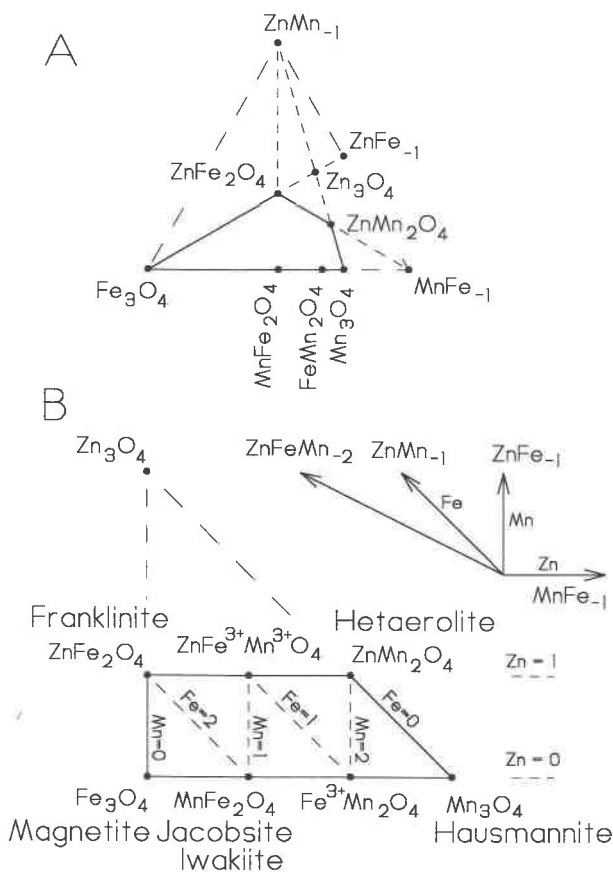
Fig. 1. Diagrams showing the composition plane of franklinite spinel, $(Zn,Mn^{2+},Fe^{2+})(Fe^{3+},Mn^{3+})_2O_4$. (A) Exchange operator or barycentric representation of the system Fe_3O_4-$MnFe_{-1}$-$ZnMn_{-1}$. (B) Exchange vector representation of compositions derived from Fe_3O_4 by the vectors $ZnFe_{-1}$ and $MnFe_{-1}$.

MINERALOGICAL EXAMPLES

Franklinite and related spinels

Exchange operators, a type of chemical component, are electrically neutral, and an operator such as $MnFe_{-1}$ can represent either $Mn^{2+}(Fe^{2+})_{-1}$ or $Mn^{3+}(Fe^{3+})_{-1}$. Mn- and Fe-bearing minerals therefore can have fewer components than one might infer from the number of named end-members, and certain "end-members" can be compositional intermediates in a solid solution series (although this does not necessarily make them invalid as mineral species).

As an example, consider spinels related to franklinite, $(Zn,Mn^{2+},Fe^{2+})(Fe^{3+},Mn^{3+})_2O_4$. The five possible oxide components are ZnO, MnO, FeO, Fe_2O_3, and Mn_2O_3. This is obviously too many components, because franklinite belongs to the four-component system Zn-Fe-Mn-O. One could name six end-members: $ZnFe_2O_4$, $ZnMn_2O_4$, $MnFe_2O_4$, $MnMn_2O_4$, $FeFe_2O_4$, and $FeMn_2O_4$. How many components does this system really have? Only three, as shown on a barycentric exchange operator representation

(Fig. 1A) that was derived following the method of Burt (1974), and a subsequent exchange vector representation (Fig. 1B). In a sense, franklinite belongs to the ternary system Fe_3O_4-Mn_3O_4-Zn_3O_4, although the last oxide composition is unstable (equivalent to a mixture of 3 ZnO and $\frac{1}{2}$ O_2), and the accessible compositions define a quadrilateral with the vertices Fe_3O_4, Mn_3O_4, $ZnMn_2O_4$, and $ZnFe_2O_4$ (e.g., Mason, 1947).

For Figure 1B, Fe_3O_4 is the additive component (Thompson, 1981, 1982); other additive components could have been used instead, and each would have generated the same diagram. Inasmuch as vector operations are commutative, the exchange operations can be applied in any order. Vector operations are also associative, so that operations such as $ZnMn_{-1}$ can be considered as $ZnFe_{-1}$, then $FeMn_{-1}$.

This diagram also illustrates two types of limits to such diagrams, chemical and crystal-chemical. Strictly chemical limits are those applied by stoichiometry alone and are, for this diagram, the limits defined by the three lines Zn = 0 (horizontal), Mn = 0 (vertical), and Fe = 0 (−45°). These define a triangle with corners Fe_3O_4, Mn_3O_4, Zn_3O_4. The last corner, although chemically attainable, must be unstable as a spinel because trivalent Zn does not exist in minerals. The three points labeled $ZnMn_{-1}$, $ZnFe_{-1}$, and $MnFe_{-1}$, are only attainable mathematically; they do not represent obtainable chemical compositions. A second, more restrictive set of limits is provided by crystal-chemical considerations. This is outlined in solid lines and here defines a quadrilateral. Examples are given below for systems in which the chemical limits alone define quadrilaterals and pentagons rather than triangles.

A vector representation such as Figure 1B would be especially useful for interpreting electron microprobe analyses of franklinite. Although valences of Mn and Fe may not be known accurately, lines of constant Mn (of any valence) are vertical and of Fe (of any valence) have a slope of −1. Lines of constant Zn are horizontal, as shown. These slopes are parallel to the slopes of the three vectors in the scaled inset labeled Mn, Fe, and Zn, respectively, according to the noninvolved elements or ions.

The basis vectors $ZnFe_{-1}$ and $MnFe_{-1}$ on Figure 1B could have been drawn at an angle other than 90° (such as 60°, forming an equilateral triangle) and could have been scaled differently. The advantage of using orthogonal basis vectors of equal length is that compositions can be plotted on ordinary graph paper. Similarly, analyses or recalculated mineral formulas, commonly recorded on an electronic spreadsheet, can be plotted on ordinary x-y diagrams (such as Zn vs. Mn in this case).

The scaled inset diagram also shows the derived vector $ZnFeMn_{-2}$, which represents a possible coupled substitution. Numerous other coupled substitutions could be derived by linear combinations of the two basis vectors $MnFe_{-1}$ and $ZnFe_{-1}$; $ZnMnFe_{-2}$, for example, would represent their sum. Note that solid solution mineral compositions need not fall along such vectors unless the compositions approach a side line or some other crystal-
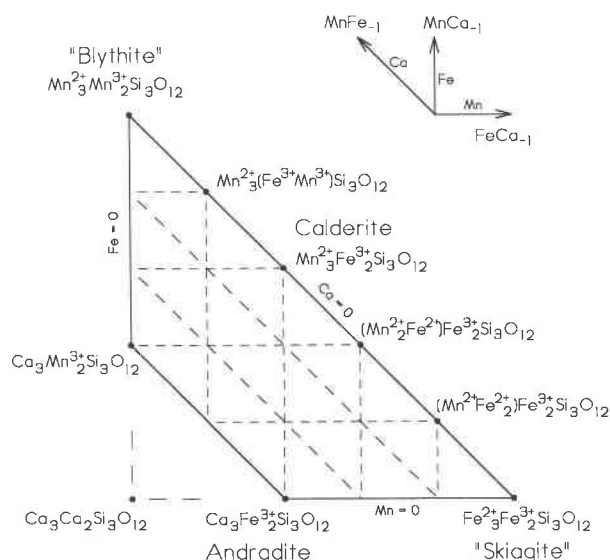
Fig. 2. Vector diagram showing the accessible composition plane of calcium manganese iron garnet, of general formula $(Ca,Mn^{2+},Fe^{2+})_3(Fe^{3+},Mn^{3+})_2Si_3O_{12}$. Compositions shown are derived from that of andradite by the basis vectors $MnCa_{-1}$ and $FeCa_{-1}$.

Fig. 3. Vector diagrams showing the composition planes for clinopyroxene, plagioclase, and melilite, using as basis vectors $Al_2(MgSi)_{-1}$ and $NaAl(CaMg)_{-1}$. (A) Clinopyroxene plane. (B) Plagioclase plane. (C) Melilite plane. See text for discussion.

chemical limit. Note also on Figure 1B that the $MnFe_2O_4$ phases jacobsite (cubic) and iwakiite (tetragonal) are compositionally only intermediates of a solid solution series between Fe_3O_4 and Mn_3O_4, although as ordered normal spinels, they are valid species (Essene and Peacor, 1983).

Garnet group

Garnets can also contain both divalent and trivalent Fe and Mn. Accessible garnet compositions derived from that of andradite using the substitutions $FeCa_{-1}$ and $MnCa_{-1}$ (and the derived substitutions $MnFe_{-1}$) are depicted on Figure 2. The composition of calderite, derived from andradite by $MnCa_{-1}$, is seen to be intermediate in a possible solid solution series between "skiagite" and "blythite" (both unknown in nature, but synthesized at high pressures, e.g., Fursenko, 1986). The compositions within the crystal-chemical limits of garnet again define a quadrilateral because the theoretical, yet chemically attainable, end-member $Ca_5Si_3O_{12}$ must be unstable as garnet (equivalent to $Ca_3Si_2O_7$ plus Ca_2SiO_4 plus ½ O_2), inasmuch as trivalent Ca is unknown.

The dashed isocomposition lines inside the quadrilateral are not labeled on this and most following figures, but from the vector inset one can see that lines of constant Fe are vertical, lines of constant Mn are horizontal, and lines of constant Ca have a slope of -1. The chemical limits of the figure are provided by the lines Mn = 0, Fe = 0, and Ca = 0; an additional limit at Ca = 3 is provided by the lack of trivalent Ca.

In general, in drawing such diagrams it is a good idea to seek all the chemical limits, which correspond to lines
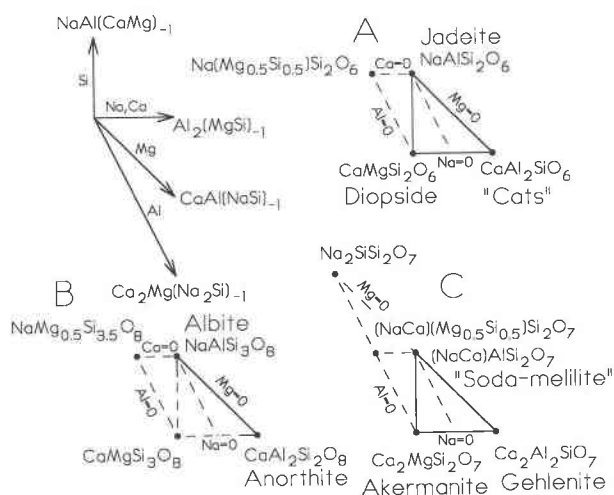
of zero content of each component. Simply applying the vectors $MnCa_{-1}$ and $MnFe_{-1}$ to the composition of andradite would have yielded the calderite and "skiagite" compositions at the corners of a triangle but would have missed the entire left side of the diagram, including two additional potential garnet end-members. The "tyranny of the triangle" would have won again.

Clinopyroxene, plagioclase, and melilite

The diagrams in Figures 1 and 2 involve relatively simple ionic substitutions, albeit for ions of variable valence. Much more complex coupled substitutions are also possible. For such cases, it is advantageous to condense the simple substitution vectors, such as $FeMg_{-1}$ and $AlFe_{-1}$; combining ions of similar ionic size and valence for graphical purposes has long been a familiar procedure. Most diagrams given below may be considered to be similarly condensed.

The same vector operations can be applied to different mineral groups. Figures 3A, 3B, and 3C show how the same exchange vectors can be applied to the formulas of diopside (clinopyroxene), albite (plagioclase), and akermanite (melilite). The vector inset shows the horizontal "Tschermak vector" $Al_2(MgSi)_{-1}$ of constant Na and Ca and the vertical vector $NaAl(CaMg)_{-1}$ of constant Si. Derived vectors of constant Mg and of constant Al, labeled on the diagram, are obtained by taking linear combinations of the basis vectors so as to eliminate Mg or Al. Similar inset vector diagrams in subsequent figures will not be discussed in the text.

Figure 3A shows how the compositions of jadeite and of "CATS" ($CaAl_2SiO_6$) can be derived from that of diopside as the corners of a triangle. The chemical limits, however, define a quadrilateral (unlike the triangles in Figs. 1 and 2), with the lines Al = 0 and Ca = 0 con-
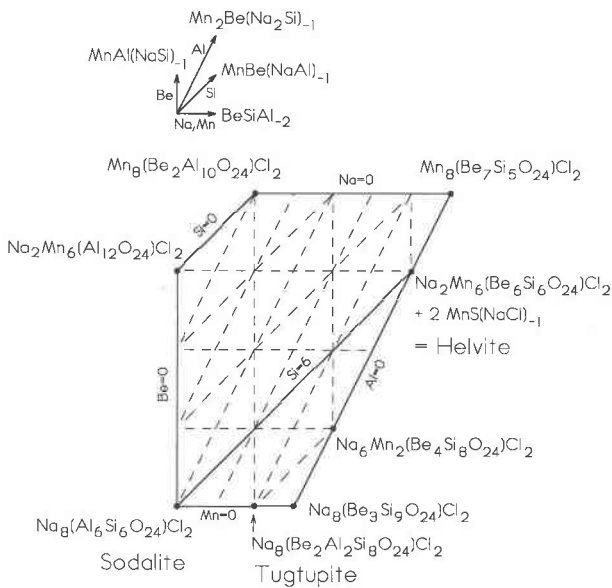
Fig. 4. Vector diagram for possible Be substitutions in the sodalite group (sodalite-tugtupite-helvite relations). The primary interest of this diagram is that its chemical limits define a pentagon. See text for discussion.

Fig. 5. Vector diagram along the line Si = 6 in the previous diagram showing sodalite-helvite relations. This is a reciprocal ternary subsystem.

verging at a fourth vertex at composition $Na(Mg_{0.5}Si_{0.5})Si_2O_6$. The presence of $^{[6]}Si$ in pyroxene is improbable, however, and the crystal-chemical limit is defined by the vertical line for Si = 2.

Figure 3B gives an analogous and congruent diagram for the chemical limits of plagioclase. The main solid solution here is between albite and anorthite; substitution of $^{[4]}Mg$ in a feldspar is difficult, although Sclar and Benimoff, 1980, have reported the synthesis of the end-member $CaMgSi_3O_8$ at 1200 °C.

Figure 3C gives a similar diagram for melilite, with gehlenite and "soda-melilite" compositions derived from the akermanite composition. The chemical limits are more extensive than for clinopyroxene or plagioclase and define a sloping triangle with an apex at the composition $Na_2SiSi_2O_7$. Such a composition with the larger tetrahedral site containing Si is somewhat improbable in melilite (Goldsmith, 1948, failed to synthesize melilites with any solid solution toward it), and the vertical line of Si = 2 again provides a crystal-chemical limit that may, however, be tentative because oxynitride melilite, $Y_2Si_3O_3N_4$, does have three Si (Fukuhara, 1988).

Be in the sodalite group

Numerous natural and synthetic phases isostructural with sodalite are listed by Hassan and Buseck (1989; cf. Hassan and Grundy, 1984, 1985). Such a long list provides many opportunities for application of exchange vectors, but one example involving Be is illustrative. The formula of tugtupite can be derived from that of sodalite by double application of the vector $BeSiAl_{-2}$, which only affects tetrahedral sites. Helvite, on the other hand, although iso-
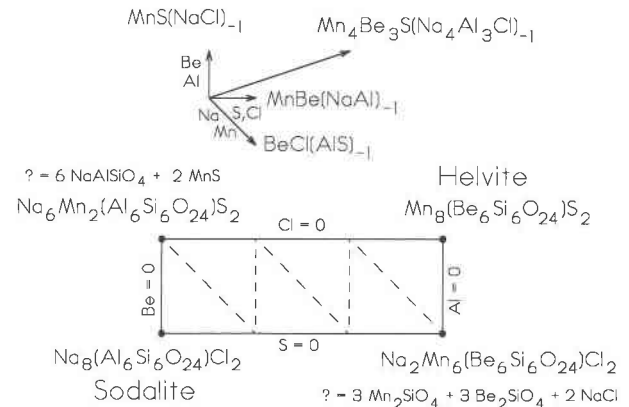
structural with sodalite, only shares Si in common with it. Figure 4 represents an attempt to relate these two Be-bearing sodalite structures.

On Figure 4, the horizontal vector is $BeSiAl_{-2}$ and the vertical vector is $MnAl(NaSi)_{-1}$, related to the plagioclase substitution by the vector $MnCa_{-1}$. The Ca analogue of this vector diagram could be used to model Be substitution in plagioclase. When these vectors are applied to the composition of sodalite, the pentagonal figure at the bottom results. It is doubtful whether many of the compositions shown are stable with the sodalite structure, although there is no obvious reason other than dissimilarities between Na and Mn why they should not be. Hassan and Buseck (1989) list Si-free aluminate phases with the sodalite structure. The chemical and crystal-chemical boundaries coincide in Figure 4, and they define a composition plane with five sides for zero values of each of the five elements Na, Be, Mn, Al, and Si. Such pentagons are not uncommon in the vector world of mineral compositions; Burt (1989b) gives examples involving the compositions of apatite, pyrochlore, and chevkinite/perrierite.

On Figure 4 the Si = 6 line along the vector $MnBe(NaAl)_{-1}$ joins sodalite to a composition close to that of helvite, $Mn_8(Be_6Si_6O_{24})S_2$, and related to it by the vector $2 MnS(NaCl)_{-1}$, as labeled. This relation is also indicated on Figure 5, which is a reciprocal ternary subsystem. The compositions at the upper left and lower right of the rectangle are probably unstable as sodalite structures, as indicated. Helvite is related to sodalite by the rather complex vector $Mn_4Be_3S(Na_4Al_3Cl)_{-1}$, which is also derived simply by subtracting the formula of sodalite from that of helvite. Working through this exercise in reverse shows how such a complex vector can be resolved into simpler ones.

Space does not permit additional or more complex examples; others, reviewed by Černý and Burt (1984) and Burt (1988, 1989a, 1989b), involve H gain or loss from hydrous phases, vacancies, and interstitials and present diagrams for which the number of anions is not constant.

Summary of features

Vector diagrams can be plotted on ordinary orthogonal graph paper or using the standard x-y plotting routines available in electronic spreadsheet programs. The formula contents of individual phases are plotted directly, without the need for a barycentric recalculation. Lines of equal contents of other ions can be determined from the scaled vector inset that should accompany each vector diagram (or x-y plot). Basis vectors can be varied according to the data available.

Exchange vectors are electrically neutral and valence insensitive; this fact can allow some apparently complex composition spaces to be plotted on a plane. Examples given above involve Mn and Fe-bearing spinels (franklinite-related compositions) and garnet (andradite-related compositions). See Burt (1988) for a similar example involving annite. The valence insensitivity of exchange vectors on mixed-valence diagrams may also be useful for plotting microprobe analyses.

On the other hand, compositions conventionally plotted on a triangle may be more correctly plotted as a condensed vector space. See the vector section of Černý and Burt (1984) for an example involving the lithium iron aluminum micas and Burt (1989b) for an example involving the isostructural alunite, beudantite, and crandallite groups.

Vectors are additive. A complex substitution vector can therefore be expressed as the sum of simpler ones (as above, for sodalite-helvite relations). Any convenient combination of simple independent exchange vectors can be applied in any order to arrive at a complex actual mineral composition.

Vector diagrams commonly reveal hypothetical endmembers which can be sought in nature or by experiment in order to discover the compositional limits of a given structure type. An example is given for the sodalite group with up to five chemically determined vertices in a plane.

The boundaries of vector diagrams can be both chemical as determined by stoichiometry (i.e., lines of zero content of individual elements or ions) and crystal-chemical as determined by valence and ionic radius (i.e., lines representing additional constraints such as lack of trivalent Zn or of octahedral Si or of tetrahedral Mg). The chemical boundaries may reveal important parts of the diagram, which otherwise might be overlooked.

Unless compositions lie very close to a line determined by chemical or crystal-chemical considerations, the composition of a mineralogical solid solution is not necessarily constrained to vary along a single vector, although it may do so to a first approximation. Looking for a unique "substitution vector" in some minerals may be a pointless exercise, unless account is taken of the compositions of coexisting minerals and fluids.

References cited

Bragg, W.L. (1937) Atomic structure of minerals. Cornell University Press, Ithaca, New York.

Bragg, W.L., Claringbull, G.F., and Taylor, W.H. (1965) Crystal structures of minerals. Cornell University Press, Ithaca, New York.

Burt, D.M. (1974) Concepts of acidity and basicity in petrology—The exchange operator approach (extended abs.). Geological Society of America Abstracts with Programs, 6, 674–676.

——— (1979) Exchange operators, acids, and bases. In V.A. Zharikov, W.I. Fonarev, and S.P. Korkovskii, Eds., Ocherki Fiziko-Khimicheskoi Petrologii (Problems in Physico-Chemical Petrology), p. 3–15. Nauka Press, Moscow (in Russian).

——— (1988) Vector representation of phyllosilicate compositions. In Mineralogical Society of America Reviews in Mineralogy, 19, 561–599.

——— (1989a) Vector representation of tourmaline compositions. American Mineralogist, 74, 826–839.

——— (1989b) Compositional and phase relations among rare earth element minerals. In Mineralogical Society of American Reviews in Mineralogy, 21, 259–307.

Černý, P., and Burt, D.M. (1984) Paragenesis, crystallochemical characteristics, and geochemical evolution of micas in granitic pegmatites. In Mineralogical Society of America Reviews in Mineralogy, 13, 257–297.

Essene, E.J., and Peacor, D.R. (1983) Crystal chemistry and petrology of coexisting galaxite and jacobsite and other spinel solutions and solvi. American Mineralogist, 68, 449–455.

Fukuhara, M. (1988) Phase relations in the Si_3N_4-rich portion of the Si_3N_4-AlN-Al_2O_3-Y_2O_3 system. Journal of the American Ceramic Society, 71, C359–C361.

Fursenko, B.A. (1986) Synthesis and stability of unusual endmembers of silicate garnets (review). International Mineralogical Association Abstracts with Programs, 107.

Gibbs, J.W. (1906, reprinted 1961) The scientific papers of J. Willard Gibbs, vol. 1: Thermodynamics. Dover Publiations, New York.

Goldsmith, J.R. (1948) Some melilite solid solutions. Journal of Geology, 56, 437–447.

Hassan, I., and Buseck, P.R. (1989) Incommensurate-modulated structure of nosean, a sodalite-group mineral. American Mineralogist, 74, 394–410.

Hassan, I., and Grundy, H.D. (1984) The crystal structures of sodalite-group minerals. Acta Crystallographica, B40, 6–13.

——— (1985) The crystal structures of helvite-group minerals, $(Mn,Fe,Zn)_8(Be_6Si_6O_{24})S_2$. American Mineralogist, 70, 186–192.

Hoffmann, B. (1966, reprinted 1975) About vectors. Dover Publications, New York.

Lewis, G.N. (1938) Acids and bases. Journal of the Franklin Institute, 226, 293–313.

Mason, B. (1947) Mineralogical aspects of the system Fe_3O_4-Mn_3O_4-$ZnMn_2O_4$-$ZnFe_2O_4$. American Mineralogist, 32, 426–511.

Sclar, C.B., and Benimoff, A.I. (1980) Magnesium in anorthite: Synthesis and petrological significance of $CaMgSi_3O_8$. Eos, 61, 392.

Smith, J.V. (1959) Graphical representation of amphibole compositions. American Mineralogist, 44, 437–440.

Thompson, J.B., Jr. (1981) An introduction to the mineralogy and petrology of the biopyriboles. In Mineralogical Society of America Reviews in Mineralogy, 9A, 141–188.

——— (1982) Compositiion space: An algebraic and geometric approach. In Mineralogical Society of America Reviews in Mineralogy, 10, 1–31.

Zen, E-An (1966) Construction of pressure-temperature diagrams for multicomponent systems after the method of Schreinemakers—A geometric approach. U.S. Geological Survey Bulletin 1225.